

Components for the X-ray radiometry beamline at BESSY II

M. Krumrey,* C. Herrmann, P. Müller and G. Ulm

Physikalisch-Technische Bundesanstalt, Abbestr. 2-12, D-10587 Berlin, Germany. E-mail: krumrey@ptb.de

(Received 4 August 1997; accepted 28 October 1997)

Optical components for the X-ray radiometry beamline of the Physikalisch-Technische Bundesanstalt at BESSY II were investigated at BESSY I. Reflectometry measurements on different mirror coatings were used to calculate their capability to suppress higher-order radiation. An MgF_2 coating proved to be best suited for photon energies below 4 keV. The reflectance of silicon (111) monochromator crystals at low photon energies around 2 keV was homogeneous within $\pm 1\%$. In a test at a superconducting wavelength shifter the cooling system for the first crystal was shown to cope with the absorbed power of 14 W.

Keywords: X-ray radiometry; mirror coatings; crystal cooling.

1. Introduction

For many applications in X-ray astronomy and technology the efficiency of detectors, the transmittance of filters or the reflectance of mirrors or crystals has to be known with an uncertainty on the 1% level. The Physikalisch-Technische Bundesanstalt (PTB), the national metrology institute of Germany, performs such radiometric calibrations using monochromatic radiation at photon energies up to 1.75 keV in its own radiometry laboratory at BESSY I (Ulm & Wende, 1995). To extend the usable range up to 10 keV, a bending-magnet beamline is being installed at the new electron storage ring BESSY II. The characteristic energy at BESSY II will be 2.5 keV, compared with 0.64 keV at BESSY I.

For the radiometric applications mentioned above the following properties are crucial:

- high spectral purity,
- high reproducibility and stability of the photon flux,
- high spectral resolution, and
- sufficient radiant power to operate a cryogenic electrical substitution radiometer (ESR) as a primary detector standard with low uncertainties (Rabus *et al.*, 1997).

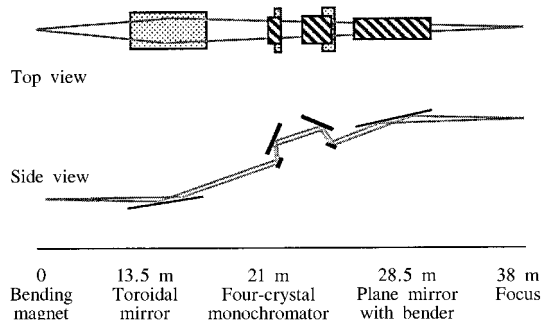


Figure 1
Layout of the beamline.

This paper briefly summarizes the layout of the beamline, already described elsewhere (Krumrey, 1998), and reports on the tests on mirror coatings and crystal performance at low energies, as well as on the thermal stability.

2. Beamline layout

In order to achieve the required reproducibility in photon energy scans, monochromatization and focusing are completely decoupled. A toroidal mirror focuses the beam in the horizontal plane and collimates it in the vertical plane (Fig. 1). A flat mirror behind the monochromator can be bent down to a radius of 2 km to superpose the vertical and the horizontal focus. The monochromator is a four-crystal device, as first proposed by DuMond (1937). It provides a fixed exit beam without crystal translations; the photon energy is scanned by two precisely controllable rotations. The corresponding motors and encoders are outside the vacuum, and the motions are transferred to UHV by differentially pumped feed-throughs. To ensure stability, the fine adjustment of the crystals is activated by in-vacuum stepper motors instead of piezo crystals.

To cover the spectral range from 1.75 to 10 keV, a set of four InSb (111) crystals and another set of four Si (111) crystals will be used. The sets can be exchanged by means of a horizontal translation, without the vacuum being broken. The spectral resolution is determined by the second and third crystal, as a result of the dispersive arrangement, not by the vertical beam divergence. The spectral purity is further increased by efficiently suppressing the rocking-curve tails.

3. Mirror coatings

Both mirrors will be used at a fixed grazing angle of 7.5 mrad. They have a Pt coating of high reflectance from 1.75 to 10 keV. The second mirror has an additional coating stripe which can be accessed by a horizontal translation of the mirror chamber. This low-energy coating should show high reflectance from 1.75 to 4 keV and low reflectance above 5.25 keV to suppress higher-order radiation from the crystal monochromator. As the second order is not allowed for the Si (111) reflection and is also very weak for InSb (111), contaminations can originate only from third- and fourth-order radiation and, therefore, have energies starting at 5.25 keV.

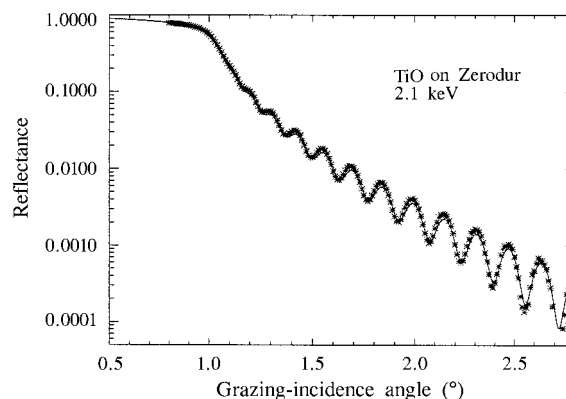


Figure 2
Measured reflectance of a TiO coating at a photon energy of 2.1 keV, together with a curve calculated with the parameters shown in Table 1.

Table 1

Calculated reflectance and suppression ratio.

The layer parameters of the low-energy coatings obtained by fitting the reflectance measurements at 2.1 keV were used to calculate the reflectance at 4 keV and the higher-order suppression ratio for a grazing incidence angle of 7.5 mrad.

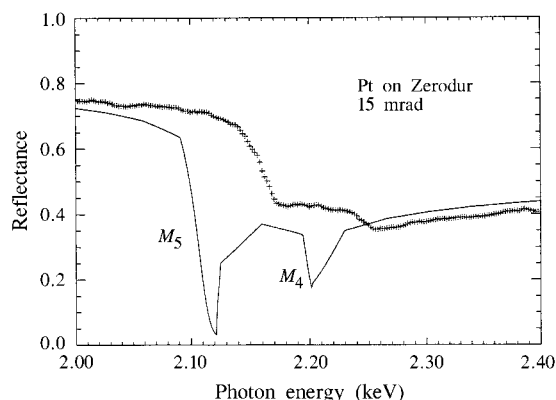
Coating	Literature density (g cm ⁻³)	Fitted density (g cm ⁻³)	Fitted thickness (nm)	Fitted roughness (Å)	Calculated reflectance at 4 keV (%)	Calculated third-order suppression ratio	
						at 1.75 keV	at 4 keV
TiO	4.9	3.7	94	14	92	6.7	2100
MgF ₂	4.26	2.8	76	15	86	9.8	2900
C	2.25	1.8	95	10	17	40	700

Several possible low-energy coatings, evaporated on Zerodur substrates, were investigated using the PTB reflectometer (Fuchs *et al.*, 1995) at the BESSY I double-crystal monochromator (DCM). For each coating the reflectance was measured as a function of the photon energy at a constant grazing angle of 15 mrad, as well as in $\theta/2\theta$ scans at a constant photon energy of 2.1 keV. The $\theta/2\theta$ scans were mainly used to determine the parameters of the coatings investigated. Fig. 2 shows the measured data and the fit for the TiO coating. For all coatings the layer density obtained was significantly lower than literature data for the bulk density (Table 1). The obtained parameters were used to calculate the higher-order suppression ratios for third-order radiation. This calculation was performed for infinitely thick layers to average over the oscillations in the reflectance, using literature data for the atomic scattering factors (Henke *et al.*, 1993). The results at two different energies together with the calculated reflectance at 4 keV and the fit parameters are listed in Table 1. The MgF₂ coating was finally chosen because it combines a high suppression ratio with a high reflectance up to 4 keV.

A platinum coating was investigated as well because literature data (Henke *et al.*, 1993) have predicted pronounced dips in the reflectance at the M absorption edges. The measured data show that there are only smooth variations of the reflectance in that spectral region (Fig. 3). The M_5 and M_4 edges are shifted to higher energies by about 40 eV. Similar results have been published by Blake *et al.* (1994) for the M edges of Ir, Pt and Au.

4. Crystal characterization

Together with the mirrors, the monochromator is the most important component of the beamline. To be able to test the four-crystal monochromator mechanics using an electronic auto-collimator instead of X-rays, the diffracting surfaces of the Si

**Figure 3**

Measured reflectance of a Pt coating at a grazing angle of 15 mrad, together with a curve calculated with the data from Henke *et al.* (1993).

crystals were polished to achieve an optical quality of $\lambda/8$. The flatness was verified with a long-trace profiler. The X-ray properties were investigated at 8.048 keV with Cu $K\alpha$ radiation using an asymmetric Si (111) monochromator crystal and a diffractometer. These instruments are part of the BESSY II optics laboratory. For the spectral range from 2.1 to 4 keV the PTB reflectometer was used at the BESSY I-DCM. From grazing-incidence-reflectance measurements at 2.1 keV a surface roughness below 10 Å was obtained, in agreement with measurements at an interference microscope.

The flatness of the crystal lattice planes was checked by taking rocking curves every 3 mm on a crystal 45 mm in length. Except for an edge region of 4 mm on each side, the maxima coincide within one tenth of the rocking-curve width. In agreement with calculations, this width was found to be around 100 arcsec at 2.1 keV and 8 arcsec at 8 keV. The corresponding peak reflectances were 34% and 85%, respectively. The peak reflectance at 2.1 keV, where the diffraction takes place very close to the surface, is homogeneous within $\pm 1\%$.

One of the crystals was etched again after optical polishing. No differences were found in the rocking curves. It can therefore be concluded that polishing did not introduce disturbing crystal lattice deformations near the surface.

5. Thermal stability test at a wavelength shifter

Especially for detector calibration the ratio of the monochromatic photon flux Φ to the storage ring current I_r should be independent of I_r and hence of the power absorbed in the first crystal. To calibrate, for example, a photon-counting device such as an Si(Li) detector, I_r will be in the nA range, while it will be around 100 mA to determine Φ/I_r , with the ESR. The maximum power absorbed by the first crystal at BESSY II will be about 20 W. The thermal stability is dominated by the cooling of the first crystal. The crystal is clamped to a copper block with an InGa layer to improve the thermal contact. The copper block is water-cooled by a closed-circuit thermostat, controlled by a Pt 100 thermo-resistor inside the crystal.

To test the cooling system before the start of BESSY II, an experiment was set up at the BESSY I wavelength shifter (WLS), which provides the same spectrum when operated at 5.75 T. At a distance of 10 m from the source, the first crystal accepts 3.5 mrad in the horizontal and 0.8 mrad in the vertical plane. The radiant power of the WLS radiation in this range was calculated to be 3 W for $I_r = 100$ mA, corresponding to an irradiance of 1 W cm⁻². The white beam from the WLS impinges directly on the first crystal, set to a fixed Bragg angle of 45°. The diffracted beam passes through a 500 μ m Be window before hitting the second crystal outside the vacuum at the same angle in the non-dispersive configuration. Rocking curves were registered with a

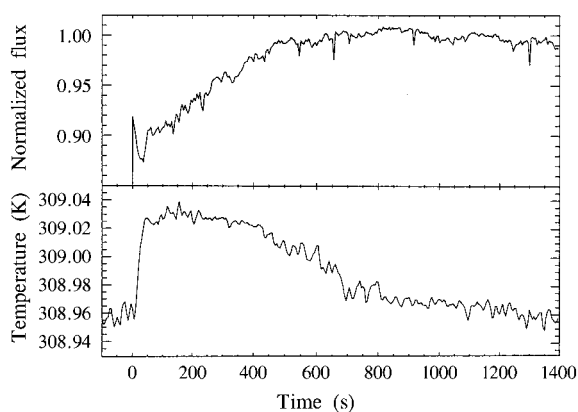


Figure 4
Temperature measured inside the crystal and normalized photon flux as a function of time after opening of the beam shutter.

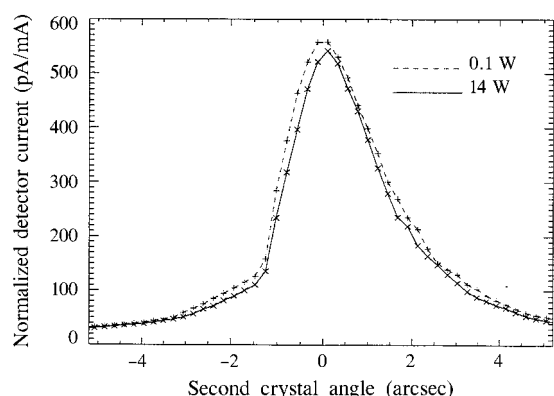


Figure 5
Si (333) rocking curves at 8.4 keV for absorbed radiant powers of 0.1 W ($I_r = 3.8$ mA) and 14 W ($I_r = 470$ mA). The detector current is normalized to the storage ring current.

photodiode by tilting the second crystal. In addition, to ensure high sensitivity to small thermal effects, a $20\ \mu\text{m}$ Cu foil was placed in front of the detector so that only the Si (333) reflection at 8.4 keV is detected. The calculated width of this rocking curve is 2.7 arcsec. The (111) reflection for the same Bragg angle with a rocking-curve width of 40 arcsec is completely absorbed in the filter. The (222) reflection is not allowed, and the contribution from the (444) reflection at 11.2 keV is below 5%.

When the beam shutter is opened, the crystal temperature increases by about $35\ \text{mK W}^{-1}$ absorbed radiant power. This low value is due to the good thermal contact provided by the InGa layer; without this layer an increase of $7\ \text{K W}^{-1}$ was observed. A

temperature change corresponds to a shift of the rocking curve, leading to a change in the detector current at fixed crystal positions. Fig. 4 shows the temperature and the normalized photon flux when the beam shutter is opened at $I_r = 60$ mA. The temperature increase of 70 mK corresponds to a reduction in flux of about 10%. After 15 min, the temperature stabilizes at its initial value; the same is true for the normalized photon flux.

Rocking curves measured at two different currents I_r are shown in Fig. 5. The currents of 3.8 and 470 mA correspond to absorbed powers of 0.1 and 14 W, respectively. The crystal temperature in both cases is 309.0 K; thus the maxima coincide. The FWHM of 2.7 arcsec agrees with the value obtained by a complete integration in the DuMond diagram. As no broadening is found even for the Si (333) reflection, it can be concluded that indirect cooling is sufficient to avoid thermal effects at the envisaged absorbed power level.

6. Conclusions

The properties of the major optical components for the X-ray radiometry beamline at BESSY II were tested with and without synchrotron radiation. An MgF_2 coating was found to be efficient for higher-order suppression in the lower part of the energy range of interest up to 4 keV. Si (111) rocking curves at low energies (2.1 keV) are not affected by polishing the crystal surface to optical quality. The reflectance is homogeneous within $\pm 1\%$. Indirect water cooling of the first silicon crystal was shown to be sufficient for the absorbed power of 14 W. As the mechanical components were also fabricated and tested, the beamline will be put into operation together with the storage ring in summer 1998.

The contributions by Michael Bock (PTB), Alexei Erko, Heiner Lammert and Markus Veldkamp (BESSY), as well as B. Gänswein (Carl Zeiss), are gratefully acknowledged.

References

- Blake, R. L., Davis, J. C., Graessle, D. E., Burbine, T. H. & Gullikson, E. M. (1994). *Resonant Anomalous X-ray Scattering*, edited by G. Materlik, C. J. Sparks & K. Fischer, pp. 79–90. Amsterdam: Elsevier.
- DuMond, J. W. M. (1937). *Phys. Rev.* **52**, 872–883.
- Fuchs, D., Krumrey, M., Müller, P., Scholze, F. & Ulm, G. (1995). *Rev. Sci. Instrum.* **66**, 2248–2250.
- Henke, B. L., Gullikson, E. M. & Davis, J. C. (1993). *At. Data Nucl. Data Tables*, **54**, 181–342.
- Krumrey, M. (1998). *J. Synchrotron Rad.* **5**, 6–9.
- Rabus, H., Persch, V. & Ulm, G. (1997). *Appl. Opt.* **36**, 5421–5440.
- Ulm, G. & Wende, B. (1995). *Rev. Sci. Instrum.* **66**, 2244–2247.